Published in final edited form as:
Am J Physiol Heart Circ Physiol. 2007 July ; 293(1): H503–H513. doi:10.1152/ajpheart.01060.2006.

Interaction between spiral and paced waves in cardiac tissue

Konstantin Agladze[1], **Matthew W. Kay**[1], **Valentin Krinsky**[2], and **Narine Sarvazyan**[1]
[1]The George Washington University, Washington DC

[2]Institut Non-Lineaire de Nice, Valbonne, France

Abstract

For prevention of lethal arrhythmias, patients at risk receive implantable cardioverter-defibrillators, which use high-frequency antitachycardia pacing (ATP) to convert tachycardias to a normal rhythm. One of the suggested ATP mechanisms involves paced-induced drift of rotating waves followed by their collision with the boundary of excitable tissue. This study provides direct experimental evidence of this mechanism. In monolayers of neonatal rat cardiomyocytes in which rotating waves of activity were initiated by premature stimuli, we used the Ca^{2}+-sensitive indicator fluo 4 to observe propagating wave patterns. The interaction of the spiral tip with a paced wave was then monitored at a high spatial resolution. In the course of the experiments, we observed spiral wave pinning to local heterogeneities within the myocyte layer. High-frequency pacing led, in a majority of cases, to successful termination of spiral activity. Our data show that *1*) stable spiral waves in cardiac monolayers tend to be pinned to local heterogeneities or areas of altered conduction, *2*) overdrive pacing can shift a rotating wave from its original site, and *3*) the wave break, formed as a result of interaction between the spiral tip and a paced wave front, moves by a paced-induced drift mechanism to an area where it may become unstable or collide with a boundary. The data were complemented by numerical simulations, which was used to further analyze experimentally observed behavior.

Keywords

antitachycardia pacing; spiral wave drift; neonatal rat cardiomyocytes

Rotating waves of activity have been discovered in many biological, physical, and chemical systems (1,3,21,39), yet these studies, in major part, were inspired by the relevance of this topic to the functioning of the heart (28,31,39). A large body of work during the past four decades using experimental and numerical approaches (for review see Refs. 25 and 38) provide a bulk of the information about the dynamics of rotating waves in heart tissue. The development of potentiometric and Ca^{2}+-sensitive indicators allowed optical mapping of excitation patterns with a high degree of spatial and temporal resolution (for review see Ref. 14). Thus it became possible not only to directly visualize spiral waves in the heart but to follow the details of their behavior.

Another important tool was the development of an in vitro experimental system using confluent cardiomyocyte monolayers. This system has reduced structural complexity compared with the heart per se, which is an advantage when the goal is an understanding of the fundamental properties of wave propagation in cardiac tissue. It has provided a basis for

Address for reprint requests and other correspondence: K. Agladze or N. Sarvazyan, Pharmacology and Physiology Dept., The George Washington Univ., 2300 Eye St., Washington, DC 20037 (phynas@gwumc.edu)..

many successful studies of wave propagation at the cellular level (19,30,35), generation of steadily rotating single and multiple-armed spiral waves (8,15), creation of controlled inhomogeneities and simulated defibrillation shocks (18), and propagation disturbances caused by local ischemia-reperfusion injury (6,33).

Rotating waves, or reentries, are believed to be responsible for many dangerous cardiac tachyarrhythmias. However, despite the wide clinical use of antitachycardia pacing (ATP), the mechanism of its success is not completely understood and remains an area of active investigation (9,12,26,34). There are two main reasons for this. *1*) Predicting propagation patterns in an intact organ is an arduous task, especially when the anatomic and functional complexity of a diseased heart is considered. *2*) Technical challenges are involved in recording propagation patterns in an intact organ at temporal and spatial resolution sufficient to reveal the interactions of rotating waves and paced wave fronts. For these reasons, our understanding of the mechanisms of reentry termination by an external source is derived, in large part, from numerical studies or simplified models of cardiac tissue (20,23,28,37,40-42). These works considered the effects of pacing on reentrant activity or provided insights regarding the motion of a spiral tip, which is relevant to the notion of paced-induced spiral drift as a potential mechanism of ATP.

The usefulness of neonatal myocyte cultures for ATP analysis was reinforced by a recent study that addressed the relationship between the steepness of the restitution curve and the ability of overdrive pacing to convert a single loop of functional reentry to multiple-arm spirals (9). This conversion, detrimental in the clinical sense, occurred in <15% of the cases; in the majority (>80%) of cases, functional reentry was successfully terminated by overdrive pacing. Notably, the exact mechanism of such termination remained unclear, mainly because of the lack of spatial resolution required to track the motion of a spiral tip.

We met this challenge by real-time observation of excitation waves using confocal microscopy. The spatiotemporal resolution of the recordings was sufficient for tracking the trajectory of a spiral wave tip in an interactive mode. Using this method, we visualized the interaction of a spiral wave tip with the wave front of paced waves. Our data suggest that *1*) stable spiral waves in cardiac monolayers tend to be pinned to local micro-heterogeneities, *2*) overdrive pacing can shift a rotating wave from its original site, and *3*) the wave break, formed as a result of interaction between the spiral tip and the paced wave front, can be moved by a pace-induced drift mechanism to an area where it becomes unstable or collides with a boundary.

METHODS

Cell preparation

Neonatal rat ventricular cardiomyocytes were obtained using a standard trypsin-collagenase digestion protocol (4). The cells were plated on 25-mm laminin-coated glass coverslips (10^5 cells/cm^2) and kept under standard culture conditions in DMEM supplemented with 5% FBS, 10 U/ml penicillin, 10 μg/ml gentamicin, and 1 μg/ml streptomycin. By the third day, the cells had formed interconnected confluent networks that exhibited rhythmic, spontaneous contractions. The cells were used in experiments during the next 3- 4 days. To monitor the monolayer activity, we loaded the cells with the Ca^{2+}-sensitive indicator fluo 4 (dissociation constant = 345 nM) and visualized excitation wave propagation by following Ca^{2+} transients, as described previously (5).

Protocols for pacing and spiral wave generation

Functional reentries (also called spiral waves) were initiated by premature stimulation, whereby two current pulses were sequentially delivered, each to a separate bipolar platinum

electrode placed in close contact with the cell layer using a micromanipulator. The time delay between the pulses placed the second pulse within the vulnerable window, creating a spiral wave. Overdrive pacing was then applied via either of the two bipolar electrodes.

To slow wave propagation, we lowered the temperature of the bathing medium to 20°C and applied the gap-junctional uncoupler heptanol (33). The diminished conduction velocity *1*) allowed the trajectory of the spiral tip to be resolved at 16 frames/s and *2*) increased the space scale of our monolayers (i.e., reduced the ratio of reentrant path length to the size of the media), such that paced waves and fully developed spiral waves could coexist. Specifically, the slow conduction velocity reduced the wavelength to ~4 mm or approximately one-sixth of the coverslip diameter, allowing observation of interactions between paced waves and fully developed spiral waves within a 25-mm coverslip.

We performed >100 individual experiments in the following order. First, we optimized a protocol for initiating the spirals. Then we determined how many of these induced spirals are stable enough for the pacing protocol and evaluated how successfully pacing terminated the stable spirals. Only then did we proceed with our efforts to visualize paced-induced drift. This was documented in 10 cases using recordings in which all of the following 4 conditions were met: *1*) the spiral shifted upon pacing; *2*) the field of view was constant; i.e., the frame was not moved; *3*) the spiral tip's trajectory was within the frame; and *4*) the interaction of paced fronts with the wave break could be seen.

Imaging techniques

For close-up measurements, the excitation waves were monitored using a confocal imaging system (LSM 510, Zeiss). Images were acquired with a ×4 magnification, 0.16 NA objective (Olympus UPlanApo) at 16 frames/s, 64 × 64 pixels, and 30 μm/pixel spatial resolution. Fluo 4 was excited at 488 nm using a 25-mW argon laser, and emission was acquired from 505–530-nm range. The sensitivity of the confocal system allowed us to observe Ca^{2+} transients in real time, thereby enabling us to acquire the data while moving the field of view and pacing the layer.

The downside of confocal imaging is its limited field of view, which was circumvented with a charge-coupled device camera imaging system, which we used to image the entire coverslip. In this system, an Andor iXon DV860DCS-BV camera (100 frames/s, 64 × 64 pixels after 2 × 2 binning, and 0.5 mm/pixel spatial resolution) was fitted with a 6 mm/F1.0 lens (Cosmicar C40601) and close-up lenses (+17, Kodak). Excitation light was supplied by two light-emitting diodes (Luxeon V Star, 470 nm), each of which was coupled to a fiber-optic guide to direct light onto the coverslip.

The tile mode of the confocal imaging system (LSM 510, Zeiss) was employed to create Fig. 2. The motorized stage of the confocal imaging system was used to stitch together multiple individual frames, each at a high spatial resolution.

Numerical simulations

Spiral waves and paced planar waves were simulated using a continuous isotropic sheet model with no-flux boundary conditions (27). Transmembrane potential (V_m) was computed at each node in a rectilinear grid as

$$\frac{\partial V_m}{\partial t} = D\nabla^2 V_m - \frac{I_{ion}}{C_m}$$

with a membrane capacitance (C_m) of 1.0 μF/cm^2. The membrane current (I_{ion}; μA/cm^2) kinetics were computed using the Drouhard-Roberge formulation (13) of the inward Na^+ current (I_{Na}) and the Beeler-Reuter formulations (7) of the slow inward current (I_s), time-independent K^+ current (I_{K1}), and time-activated outward current (I_{x1}). To obtain sustained spiral waves without breakup, the time constants of Ca^{2+} current activation and inactivation were slowed by multiplying by a factor σ, as previously described (11,27).

Model parameters were as follows: the grid size was 2.5 × 2.5 mm, dx = 0.025 mm, dt = 0.015 ms, D = 0.6 mm^2/s, and σ = 0.50. A spiral was initiated by cross-field stimulation. In the absence of a local heterogeneity, the spiral was not stable and drifted into a boundary. Introducing a heterogeneity captured and stabilized the spiral. The process of spiral "capture" is illustrated in Fig. 3 (online Supplement 1). Specifically, the spiral was first initiated by cross-field stimulation. After a small delay, a heterogeneity was introduced in the center of the grid. This was done by assigning a value of $0.3g_{K1}$ as the conductance of the time-independent outward K^+ channel for nodes within a 4-mm-radius circle from the center of the grid. Planar waves were then launched from the bottom edge of the grid at a frequency exceeding the spiral rotation rate.

RESULTS

Termination of spiral wave activity

Rotating wave initiation and termination were studied in a total of ~100 cell cultures. An individual coverslip was used several times; i.e., after termination of the reentry, it was induced again and subjected again to high-frequency pacing. The stability of a rotating wave and the success or failure of a pacing protocol were determined from Ca^{2+} transient signals obtained from a region of interest within the field of view. After five to eight rotations, ~70% of induced reentries (28 of 39 cases) self-terminated (Fig. 1*A*). If a rotating wave persisted, the field of view was adjusted for visualization of the spiral tip, and overdrive pacing was applied. Overdrive pacing terminated spiral activity with a 90% success rate (27 of 30 cases). The trace in Fig. 1*B* shows the initiation of a spiral wave followed by a train of paced waves that successfully terminated the spiral activity. The trace in Fig. 1*C* shows a rare unsuccessful attempt to terminate spiral activity by overdrive pacing. Examples of spiral's spontaneous and paced-induced terminations are shown as online Supplements 3 and 4, respectively.

Role of heterogeneity

The heart is a highly heterogeneous organ in which rotating waves are likely to be pinned to anatomic or functional obstacles such as coronary vessels, collagen fibers, and ischemic or scar tissue (32). Cardiomyocyte cultures represent a much less heterogeneous substrate. However, the presence of fibroblasts, small differences in cell plating density, clusters of damaged or dead myocytes, and even differences in the alignment and number of intercellular junctions make this simplified model of cardiac tissue intrinsically heterogeneous. The heterogeneous nature of a monolayer is illustrated in Fig. 2, which shows a macroscopically homogeneous coverslip that was imaged with a spatial resolution sufficient for visualization of microscopic heterogeneities.

Although monolayer heterogeneities have minimal impact on planar wave propagation, they do affect spiral tip behavior, primarily because of a higher impact of the current sink-source relationship at critical curvatures. Indeed, the majority of spirals that were stable (existed for >1 min) appeared to rotate around areas of microscopic heterogeneities, such as those shown in Fig. 2. A situation of how this might happen is shown in Fig. 3, where a spiral initiated by cross-field stimulation was captured by a nearby heterogeneity (also animated in online

supplement 1). The small area with altered K^+ conductance (g_{k1}), seen as a brighter spot at the center, acts to attract and anchor the tip of the spiral wave (Fig. 3).

Interaction of the paced waves with the spiral tip: formation of a wave break

To observe the interaction of a spiral wave with paced waves, we initiated a stably rotating spiral and adjusted the field of view such that its tip was in the center. The tip was monitored for ≥1 min to confirm stability. Overdrive pacing was then applied from a distant site. Pacing continued for up to 30 s after paced waves approached the spiral tip and entrained the entire field of view. A typical pattern of the interaction of paced waves with a spiral tip is shown in Figs. 4 and 5. An activation map in Fig. 4*A* shows one complete rotation of the spiral, and a snapshot of a spiral tip is shown in Fig. 4*B*. This spiral wave was stable with a period of 0.72 s. It persisted for ≥60 s before it was terminated by overdrive pacing (online supplement 2).

A frame-by-frame sequence illustrating the collision of a spiral tip with a paced wave is shown in Fig. 4*C*. The planar front of the paced wave can be seen as it approaches the spiral tip. The last frame in the *top row* in Fig. 4*C* shows that the two waves have collided and coalesced. Propagation of the coalesced wave continued in the direction of the paced wave, but propagation into an area beyond the collision site was blocked because of refractoriness, resulting in a wave break (Fig. 4*C*, *bottom row*). Once the broken wave encountered tissue that regained excitability, it curled into a new spiral. A movie corresponding to the events shown in Fig. 4 can be found online (supplement 4). The numerical illustration of this process presented in Fig. 4*D* shows how the tip of the spiral, captured by a local heterogeneity in Fig. 3, interacts with the planar wave front of the paced wave.

Paced-induced drift of spiral waves

When the frequency of overdrive pacing exceeds the rotational frequency of the spiral, collisions between the wave front of paced waves and the spiral occur closer and closer to the tip (Fig. 5). In all 10 documented cases, spirals drifted away from the pacing site. With each paced wave, the collision site progresses toward the upper right corner until it reaches the spiral tip (Fig. 5*A*, *top row*). As shown in Fig. 5*B*, the tip location remained unchanged when the spiral collided with paced *waves 1*, *2*, and *3*, while the respective collision sites moved. When paced *wave 4* collided with the tip, local refractoriness prevented the spiral from curling into the same area, causing an upward displacement of the wave break (arrow in Fig. 5*B*). Subsequent paced *waves 5–8* continued to displace the wave break until it disappeared from of the field of view (last frame in Fig. 5*A* and online supplement 4). A numerical illustration of paced-induced drift is shown in Fig. 6. The plot and corresponding frames (full sequence can be seen in supplement 5) show the upward movement of the collision site followed by tip displacement away from the pacing electrode. The overall scenario is identical to the experimental case in Fig. 5. Paced-induced drift synchronizes the wave break with the frequency of the pacing wave.

Collision of the wave break with the boundary

Spiral waves can anchor to macroscopic obstacles to form anatomic reen-tries. The success of overdrive pacing in terminating anatomic reentries may depend on the size and boundary conditions of these obstacles (24). This study, however, focuses on functional reentries under conditions where endogenous microscopic heterogeneity simply anchors the spiral tip, thereby minimizing its meandering, but the size of the spiral core is negligible (Fig. 4*A* and online supplement 2. The complete sequence of events can be seen in online supplement 6). When a train of paced waves shifts a spiral wave from its original location, it is possible that *1*) the wave break curls into a new spiral wave, which reattaches to heterogeneity or becomes unstable and self-terminates and *2*) the wave break collides with an unexcitable

boundary. To visualize such collisions, we used a CCD camera-based imaging system to expand our field of view to capture the entire coverslip (Fig. 7). A spiral wave was situated 5 mm from the border of the coverslip and pinned to an area of depressed conduction (Fig. 7, *A* and *B*). It stably rotated for several minutes before overdrive pacing was applied. The position of the pacing electrode is marked by two black dots in Fig. 7*A*. On collision of the paced waves with the spiral, the two waves coalesced (Fig. 7, *C* and *D*). The wave break then curled into a new spiral, which remained pinned to the local heterogeneity (Fig. 7*E*). With each new paced wave, the collision site and the area where the two waves coalesced moved toward the coverslip boundary and away from the pacing electrode (Fig. 8). Ultimately, the refractoriness of the collision site prevented curling of the wave break toward the area of local heterogeneity in a manner similar to the events shown in Fig. 4. This forced the wave break to shift, collide with the boundary (Fig. 7*F*), and terminate.

DISCUSSION

ATP is a procedure that is widely used to restore normal heart rhythm without application of damaging defibrillation shocks. Despite significant experimental and theoretical effort to clarify the mechanisms of ATP, it is unclear how a sequence of high-frequency pulses terminates the rotating waves, which are believed to be a cause of tachycardia (38). The conventional explanation is that one of the ATP pulses occurs during the so-called vulnerability window (VW), generating a wave front that rotates in a direction opposite to the existing rotating wave. This newly formed retrograde wave front then follows the same path as the existing rotating wave, causing both waves to annihilate on collision. The alternative explanation involves pacing-induced displacement of rotating waves. Once shifted from their original locations, functional reentries are likely to self-terminate or collide with the media boundary. Indeed, studies in isolated swine and sheep ventricular muscle slices (12,26), as well as in monolayers of neonatal rat cardiomyocytes (9), suggested that such a scenario does occur.

Despite its importance, however, the mechanism of paced-induced spiral displacement remains unclear. This is largely due to the spatiotemporal resolution required to visualize the motion of the spiral tip. Here, using monolayers of rat ventricular myocytes in which propagation velocity was significantly reduced to resolve the motion of the spiral tip, we attempted to fill this gap. This measure also allowed us to reduce the wavelength of propagating waves to match the dimensions of our experimental preparations (25-mm coverslip). From experiments in chemical media and numerical analysis, it has been shown that when the frequency of overdrive pacing exceeds the rotational frequency of the spiral, collisions between the wave front of paced waves and the spiral approach the tip (29). This is true even when the size of the media is much larger than the wavelength, such that the spiral tip appears to be shielded from paced waves (20,23). However, wavelength estimates for cardiac tissue suggest that heart size and the wavelength are comparable (22). Thus it is unlikely that the in vivo pacing source will be shielded from the spiral core by multiple wraps of the spiral arm. Therefore, one can argue that, even in the case of a limited number of paced waves (standard ATP protocols of 7–20 pulses), their wave fronts may be able to encroach on the tip of the rotating wave, similar to the sequence shown in Fig. 5. The closer the pacing electrode is to the core of a spiral, the more likely it is that a fixed number of pacing stimuli will reach the tip.

When a paced wave encountered the tip of a spiral wave, the spiral wave condensed to a singular wave break (Fig. 4*C*), similar to the scenario reported earlier for chemically excitable media (29). If pacing was maintained, this wave break cycled through three distinct steps: *1*) it encountered excitable tissue and evolved into a spiral tip, *2*) it collided with another paced wave, and *3*) it propagated with the paced wave without evolving until it

encountered excitable tissue, at which point it again evolved into a spiral tip (*step 1*). Within this cycle, the wave break, which is the seed of the potential spiral, is gradually pushed from its original site (Fig. 5). Notably, the wave break drifts slowly compared with the propagation speed (Figs. 5 and 6).

Mechanism-based suggestions to increase ATP success rates are in high demand, since this important task remains largely empirical (36). The two alternative mechanisms of ATP, i.e., VW-based and paced-induced drift-based, offer opposite recommendations relative to pacing frequency. In the VW-based mechanism, a retrograde wave front is generated when a stimulus is placed within the partially recovered tail of the rotating wave. In this scenario, a number of pulses are needed to find a narrow VW. If T_s is the period of spiral wave rotation and T_p is the period of paced waves, then $T_s - T_p = \Delta T$ should not exceed the VW. If so, then even with arbitrary placement of the first stimulus, the time of subsequent stimuli will be systematically shifted with respect to the tail of a rotating wave, such that, with enough stimuli, one will eventually be placed within the VW. If the condition is not fulfilled, for instance, if T_p is substantially lower than T_s, then the success of placing a stimulus within the VW is probabilistic, and it is possible that the number of stimuli required for successful ATP would increase dramatically. Therefore, pacing frequency should not significantly exceed the rotational rate of reentry.

On the other hand, the velocity of paced-induced drift could be accelerated by increasing pacing frequency similar to that in the chemical active medium (2) and confirmed numerically (16). So the rotating wave is pushed away faster with increasing $T_s - T_p = \Delta T$ (the sole limitation being tissue capture). Therefore, the drift-induced pacing mechanism leads to a recommendation opposite to that derived from the VW concept.

Although the above reasoning is attractive because of the clarity of the underlying mechanisms, one warns against its simplistic interpretation. The in vivo situation is much more complex: waves propagate in three dimensions, their curvature depends on fiber orientation, and tissue properties change as ischemia sets in. In addition, multiple rotating waves can occur during one tachycardia episode, and/or paced-induced drift can be followed by VW-based termination (10).

Another factor to consider for the VW-based and paced-induced drift mechanism is the geometry and size of cardiac tissue. Stimulation into VW will terminate reentry only in a one-dimensional case or in a very confined space. Otherwise, instead of termination, the stimulus could initiate a new pair of rotating waves. Thus, limiting the excitable area is a crucial prerequisite. In the case of the drift-based termination, the border also plays a decisive role. In vivo, many anatomic structures, including large vessels, annuli of cardiac valves, and atrioventricular septa, which insulate ventricles from the atria, as well as regions of fibrotic or ischemic tissue, can serve as a boundary. In the case of three-dimensional rotating waves, or scrolls, the endocardium and epicardium also serve as boundaries of the excitable media.

Limitations

1. Because of the small field of view required to monitor spiral tip movement, it was not always possible to clearly attribute paced-induced termination of spiral waves to just the mechanism of paced-induced drift. In a few cases, only one paced-induced shift of a spiral tip resulted in a spiral's disappearance from the field of view and cessation of its activity. Therefore, the emphasis of this study is to show that paced-induced drift does occur, not on its relative prevalence. Numerical studies suggest that many factors, including the distance between the electrode and a spiral tip, propagation velocity, and the ratio of spiral to pacing frequency, may

affect the ability of a limited number of paced waves to reach the spiral tip (17,20,23). Additionally, endogenous monolayer heterogeneities will impact the success of unpinning and how drift would progress after a spiral is unpinned (24,34). We did not report mean values of drift velocity (*V*drift), as this value depends on pacing frequency. Our previous studies (29) suggest that $V_{\text{drift}} \sim V_{\text{planar wave}} \times (1 - T_s/T_p)$. Although this relationship is likely to hold for cardiac preparations, full statistical confirmation awaits future studies.

2. Although it is very likely that stably rotating spirals would be pinned to heterogeneities such as those shown in Fig. 2, further work is required to prove and quantify this effect.

3. The Beeler-Reuter model provides a generic reconstruction of the action potential for a mammalian ventricular myocardial cell. It was used in our numerical experiments to explore the interactions between paced wave fronts and the tips of spiral waves that were observed in our experiments. We shortened action potentials in our model by reducing the activation and inactivation time constants of the Ca^{2+} current. This was done to reduce the time scale of interaction events between paced wave fronts and spiral tips from ~10–15 s, as observed in experiments, to a little more than 1 s for the simulations. This substantially reduced the computational burden of our simulations. Although the time scale reduction is not expected to alter the model results, it represents one of the limitations of the present study. More detailed numerical models are needed for full exploration of the observed phenomenon.

4. Unanchored spirals in cardiomyocyte cultures can disappear because of their collision with the boundary. However, they often self-terminate without any apparent anatomic obstacle in sight. The mechanism of such self-termination remains to be addressed.

Conclusions

We have shown that overdrive pacing can terminate rotating waves by a paced-induced drift mechanism in a simple, endogenously heterogeneous model of cardiac tissue. The latter occurs via cyclical movement of wave break. Continuous high-frequency pacing then shifts the wave break to an area where the spiral becomes unstable or collides with the boundary of the excitable medium.

We also may note that the ability to directly observe paced-induced drift of rotating waves in cardiac preparations offers an important methodological tool to further understand this process, e.g., questions regarding the size of heterogeneity that stabilizes the rotating wave and/or its boundary conditions; the role of fiber anisotropy; the effects of the spiral core on the direction and velocity of paced drift; the efficacy of different pacing strategies; or a new combination of therapies that combine low-voltage shocks with overdrive pacing. All these questions can be addressed with relative ease using the described experimental approach.

Supplementary Material

Refer to Web version on PubMed Central for supplementary material.

Acknowledgments

We thank Dr. Nadezhda Agladze and Luther Swift for assistance with cardiomyocyte culture preparations.

GRANTS: This study was financially supported by National Heart, Lung, and Blood Institute Grant HL-076722 and a Biomedical Engineering Research Grant from the Whitaker Foundation.

REFERENCES

1. Agladze K, Steinbock O. Waves and vortices of rust on the surface of corroding steel. J Phys Chem A 2000;104:9816–9819.
2. Agladze KI, Krinsky V. Multi-armed vortices in an active chemical medium. Nature 1982;296:424–426.
3. Allessie MA, Bonke FI, Schopman FJ. Circus movement in rabbit atrial muscle as a mechanism of tachycardia. Circ Res 1973;33:54–62. [PubMed: 4765700]
4. Arutunyan A, Webster DR, Swift LM, Sarvazyan N. Localized injury in cardiomyocyte network: a new experimental model of ischemia-reperfusion arrhythmias. Am J Physiol Heart Circ Physiol 2001;280:H1905–H1915. [PubMed: 11247808]
5. Arutunyan A, Swift LM, Sarvazyan N. Initiation and propagation of ectopic waves: insights from an in vitro model of ischemia-reperfusion injury. Am J Physiol Heart Circ Physiol 2002;283:H741–H749. [PubMed: 12124223]
6. Arutunyan A, Pumir A, Krinsky VI, Swift LM, Sarvazyan N. Behavior of ectopic surface: effects of β-adrenergic stimulation and uncoupling. Am J Physiol Heart Circ Physiol 2003;285:H2531–H2542. [PubMed: 12893638]
7. Beeler GW, Reuter H. Reconstruction of the action potential of ventricular myocardial fibres. J Physiol 1977;268:177–210. [PubMed: 874889]
8. Bursac N, Aguel F, Tung L. Multiarm spirals in a two-dimensional cardiac substrate. Proc Natl Acad Sci USA 2004;101:15530–15534. [PubMed: 15492227]
9. Bursac N, Tung L. Acceleration of functional reentry by rapid pacing in anisotropic cardiac monolayers: formation of multi-wave functional reentries. Cardiovasc Res 2006;69:381–390. [PubMed: 16274682]
10. Byrd IA, Kay MW, Pollard AE. Interactions between paced wavefronts and monomorphic ventricular tachycardia: implications for antitachycardia pacing. J Cardiovasc Electrophysiol 2006;17:1129–1139. [PubMed: 16989652]
11. Courtemanche M, Winfree AT. Re-entract rotating waves in a Beeler-Reuter-based model of two-dimensional cardiac electrical activity. Int J Bifurcation Chaos 1991;1:431–444.
12. Davidenko JM, Salomonsz R, Pertsov AM, Baxter WT, Jalife J. Effects of pacing on stationary reentrant activity. Theoretical and experimental study. Circ Res 1995;77:1166–1179. [PubMed: 7586230]
13. Drouhard JP, Roberge FA. Revised formulation of the Hodgkin-Huxley representation of the sodium current in cardiac cells. Comput Biomed Res 1987;20:333–350. [PubMed: 3621918]
14. Efimov IR, Nikolski VP, Salama G. Optical imaging of the heart. Circ Res 2004;95:21–33. [PubMed: 15242982]
15. Entcheva E, Lu SN, Troppman RH, Sharma V, Tung L. Contact fluorescence imaging of reentry in monolayers of cultured neonatal rat ventricular myocytes. J Cardiovasc Electrophysiol 2000;11:665–676. [PubMed: 10868740]
16. Ermakova EA, Krinsky VI, Panfilov AV, Pertsov AM. Interaction between spiral and flat periodic autowaves in an active medium. Biofizika 1986;31:318–323. [PubMed: 3697394]
17. Ermakova EA, Pertsov AM. Interaction of rotating spiral waves with a boundary. Biofizika 1986;31:855–861.
18. Fast VG, Rohr S, Gillis AM, Kleber AG. Activation of cardiac tissue by extracellular electrical shocks: formation of “secondary sources” at intercellular clefts in monolayers of cultured myocytes. Circ Res 1998;82:375–385. [PubMed: 9486666]
19. Fast VG, Ideker RE. Simultaneous optical mapping of transmembrane potential and intracellular calcium in myocyte cultures. J Cardiovasc Electrophysiol 2000;11:547–556. [PubMed: 10826934]
20. Fu YQ, Zhang H, Cao Z, Zheng B, Hu G. Removal of a pinned spiral by generating target waves with a localized stimulus. Phys Rev E Stat Nonlin Soft Matter Phys 2005;72:046206. [PubMed: 16383511]
21. Gerisch G. Cell aggregation and differentiation in *Dictyostelium*. Curr Top Dev Biol 1968;3:157–197. [PubMed: 5002049]

22. Girouard SD, Rosenbaum DS. Role of wavelength adaptation in the initiation, maintenance, and pharmacologic suppression of reentry. J Cardiovasc Electrophysiol 2001;12:697–707. [PubMed: 11405405]
23. Gottwald G, Pumir A, Krinsky V. Spiral wave drift induced by stimulating wave trains. Chaos 2001;11:487–494. [PubMed: 12779486]
24. Ikeda T, Yashima M, Uchida T, Hough D, Fishbein MC, Mandel WJ, Chen PS, Karagueuzian HS. Attachment of meandering reentrant wave fronts to anatomic obstacles in the atrium. Role of the obstacle size. Circ Res 1997;81:753–764. [PubMed: 9351449]
25. Jalife J. Ventricular fibrillation: mechanisms of initiation and maintenance. Annu Rev Physiol 2000;62:25–50. [PubMed: 10845083]
26. Kamjoo K, Uchida T, Ikeda T, Fishbein MC, Garfinkel A, Weiss JN, Karagueuzian HS, Chen PS. Importance of location and timing of electrical stimuli in terminating sustained functional reentry in isolated swine ventricular tissues: evidence in support of a small reentrant circuit. Circulation 1997;96:2048–2060. [PubMed: 9323098]
27. Kay MW, Gray RA. Measuring curvature and velocity vector fields for waves of cardiac excitation in 2-D media. IEEE Trans Biomed Eng 2005;52:50–63. [PubMed: 15651564]
28. Krinsky VI. Spread of excitation in an inhomogeneous medium (state similar to cardiac fibrillation). Biophys J 1966;11:776–784.
29. Krinsky VI, Agladze KI. Interaction of rotating chemical waves. Physica D 1983;8:50–56.
30. Kucera JP, Kleber AG, Rohr S. Slow conduction in cardiac tissue: insights from optical mapping at the cellular level. J Electrocardiol 2001;34:57–64. [PubMed: 11781937]
31. Moe GK, Jalife J. Reentry and ectopic mechanisms in the genesis of arrhythmias. Arch Inst Cardiol Mex 1977;47:206–211. [PubMed: 20066]
32. Pertsov AM, Davidenko JM, Salomonsz R, Baxter WT, Jalife J. Spiral waves of excitation underlie reentrant activity in isolated cardiac muscle. Circ Res 1993;72:631–650. [PubMed: 8431989]
33. Pumir A, Arutunyan A, Krinsky V, Sarvazyan N. Genesis of ectopic waves: role of coupling, automaticity, and heterogeneity. Biophys J 2005;89:2332–2349. [PubMed: 16055545]
34. Ripplinger CM, Krinsky VI, Nikolski VP, Efimov IR. Mechanisms of unpinning and termination of ventricular tachycardia. Am J Physiol Heart Circ Physiol 2006;291:H184–H192. [PubMed: 16501014]
35. Rohr S, Scholly DM, Kleber AG. Patterned growth of neonatal rat heart cells in culture. Morphological and electrophysiological characterization. Circ Res 1991;68:114–130. [PubMed: 1984856]
36. Sweeney MO. Antitachycardia pacing for ventricular tachycardia using implantable cardioverter defibrillators. Pacing Clin Electrophysiol 2004;27:1292–1305. [PubMed: 15461721]
37. Vinston M. Interactions of spiral waves in inhomogenous excitable media. Physica D 1998;116:313–324.
38. Weiss JN, Chen PS, Wu TJ, Siegerman C, Garfinkel A. Ventricular fibrillation: new insights into mechanisms. Ann NY Acad Sci 2004;1015:122–132. [PubMed: 15201154]
39. Winfree, AT. When Time Breaks Down: The Three-Dimensional Dynamics of Chemical Waves and Cardiac Arrhythmias. Princeton University Press; Princeton, NJ: 1987.
40. Winfree AT. Alternative stable rotos in an excitable media. Physica D 1991;49:125–140.
41. Xie F, Qu Z, Weiss JN, Garfinkel A. Interactions between stable spiral waves with different frequencies in cardiac tissue. Phys Rev E 1999:59.
42. Xie F, Qu Z, Weiss JN, Garfinkel A. Coexistence of multiple spiral waves with independent frequencies in a heterogeneous excitable medium. Phys Rev E Stat Nonlin Soft Matter Phys 2001;63:031905. [PubMed: 11308676]

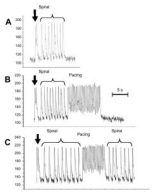

Fig. 1.

Three types of behavior observed for induced reentrant (spiral) activity. Recordings of Ca^{2+} transients are shown as relative units of fluo 4 fluorescence. Arrows indicate the application of premature stimuli, which initiated a reentrant wave. *A*: self-termination of a reentrant wave. *B*: reentrant wave termination by overdrive pacing. *C*: unsuccessful termination of reentrant wave activation by overdrive pacing.

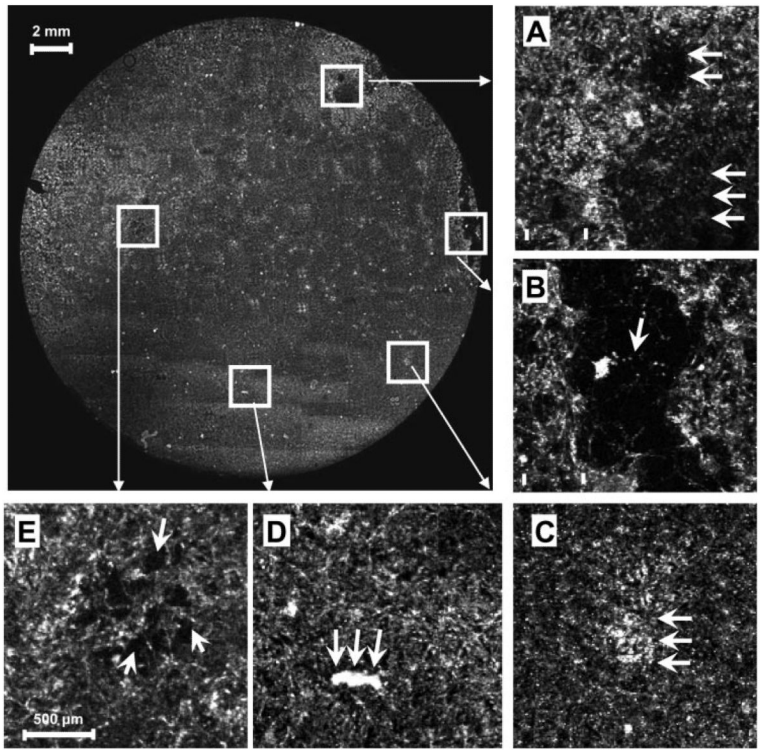

Fig. 2.

Endogenous heterogeneities in macroscopically homogenous coverslips. *A*: myocyte-free regions; *B*: mechanical damage due to forceps during coverslip transfer; *C*: areas of higher density; *D*: clusters of damaged cells on top of the monolayer (arrows); *E*: areas of lesser/uneven density.

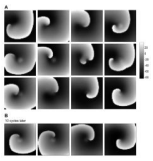

Fig. 3.

Capture of a nearby spiral by a local heterogeneity. *A*: 12 sequential frames show how a small area of heterogeneity, seen as a slightly brighter spot at the center, attracts the tip of a spiral wave. *B*: 4 sequential frames 10 cycles after the capture event shown in *A*. They illustrate that spiral remained stable and pinned to the same spot. Full sequence can be seen in the online supplement 1.

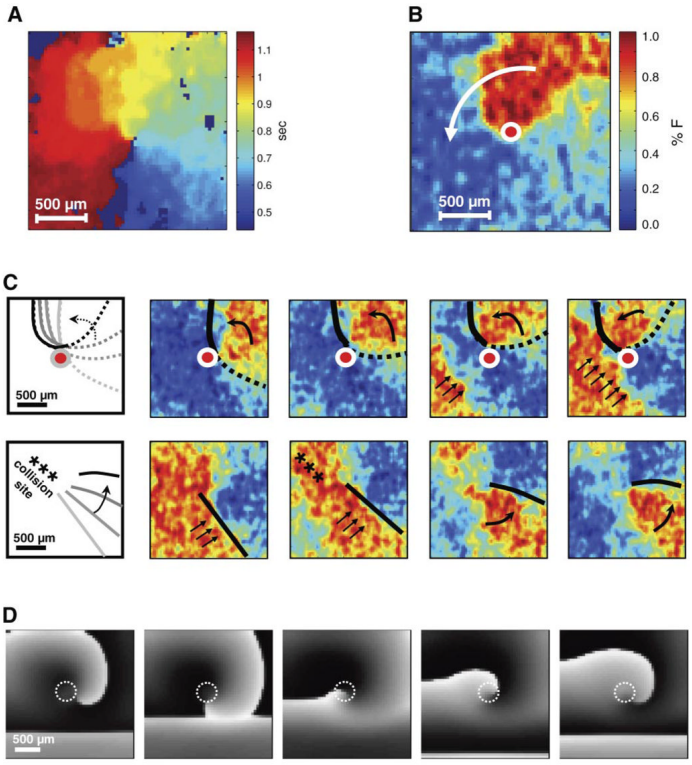

Fig. 4.

Reentrant wave terminated by rapid pacing. *A*: 1 complete rotation of the reentrant wave presented as an activation map, where color indicates time of activation at each pixel. *B*: fluorescence snapshot of the wave. Arrow denotes direction of rotation. Normalized fluo 4 fluorescence is shown in pseudocolor. Red dot indicates position of the spiral tip. *C*: sequence of frames illustrating interaction of 1 paced wave front with the tip of the spiral wave before (*top row*) and after (*bottom row*) collision. Last 2 frames show formation of a wave break. ***, Site of collision. Solid lines, wave fronts; dotted lines, wave backs. Red dot indicates position of the spiral tip. *D*: numerical illustration of the process described in *C*. Dotted circle, position of a local heterogeneity [reduced time-independent K^+ current (*I*K1)], around which the spiral rotates.

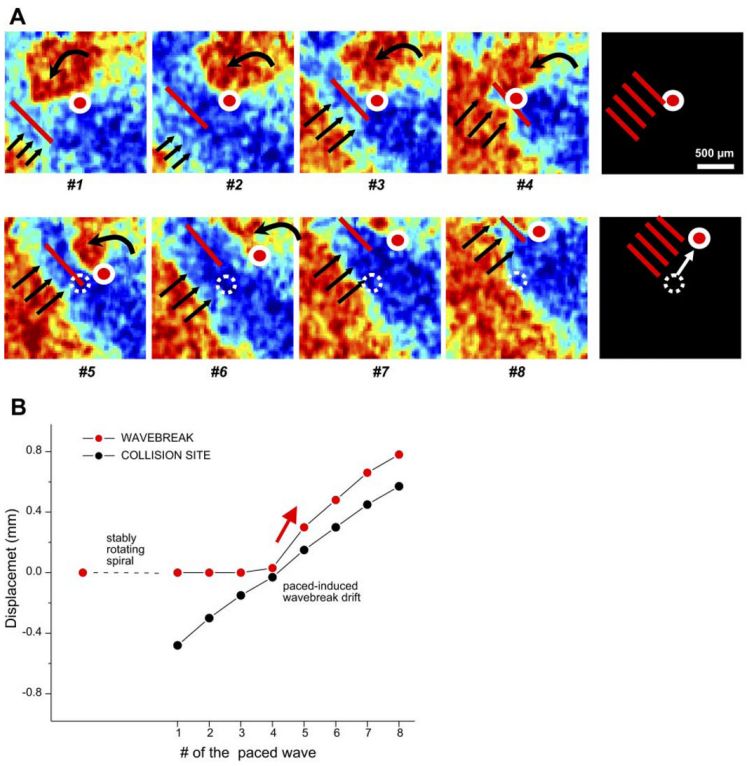

Fig. 5.

Paced-induced drift of spiral waves. *A*: impeding collisions of the spiral and 4 consecutive paced waves before they reach the tip (*top row*) and impeding collisions of the spiral wave and 4 consecutive paced waves during the paced-induced drift (*bottom row*). Arrows show direction of paced wave propagation. *Right*: relative positions of collision site (red lines) and wave break (red circle). Dotted circle indicates location of the initial wave break; arrow shows direction of paced induced drift. At this magnification (~2 × 2 mm area), individual cell heterogeneity is clearly visible. *B*: graphical illustration of process shown in *A*. Red dots, position of wave break; black dots, collision site coordinates. Displacement was measured in the direction of drift.

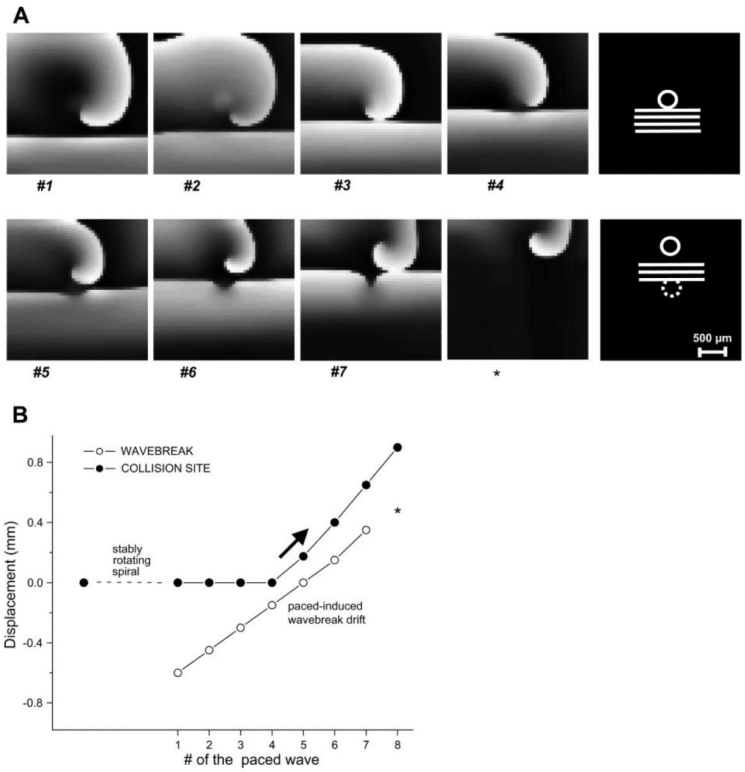

Fig. 6.

Paced-induced drift of spiral wave: numerical study. *A*: impeding collisions between the spiral wave and 4 consecutive paced waves before they reach the tip (*top row*) and 3 impeding collisions of the spiral wave and paced waves during paced-induced drift (*bottom row*). *Right*: relative positions of collision site (white lines) and wave break (solid circle). Dotted circle, area of local heterogeneity similar to that in Fig. 4*D*. *B*: graphical illustration of the process in *A*. ○, Position of the wave break; ●, collision site coordinates. *, Illustration that the wavebreak displacement occurs as a result of the previous collision (paced *wave 7*), and not due to the collision with what will be the next paced wave (*wave 8*).

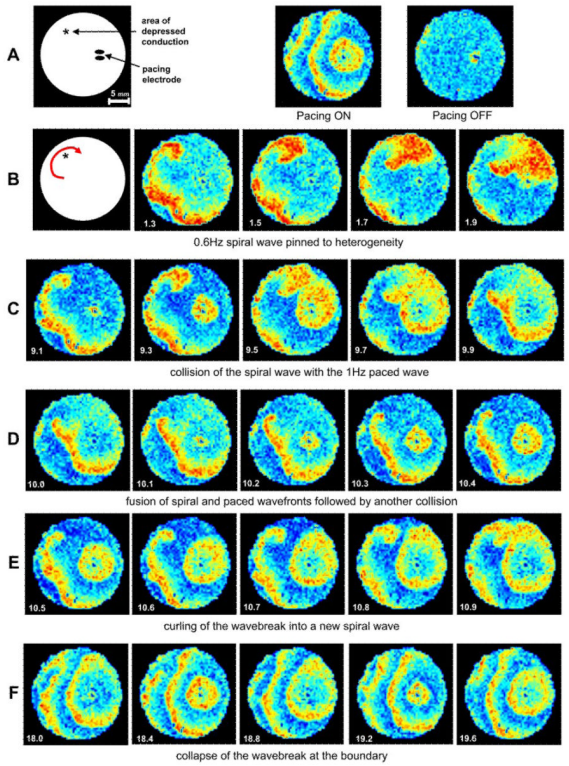

Fig. 7.

Paced-induced spiral wave detachment and subsequent termination due to wave break collision with a boundary. *A*: location of pacing electrodes and a local heterogeneity (*left*) and circular wave fronts of paced waves (note changes in wave curvature near local heterogeneity) and appearance of the cell layer after overdrive pacing was turned off (*right*). *B*: 4 sequential frames showing spiral wave pinned to a heterogeneity. *C*: 5 sequential frames showing collision of the spiral wave with the paced wave. *D*: 5 sequential frames showing the 2 waves coalescing into a single wave front. *E*: 5 sequential frames showing curling of the wave break into a new spiral wave. *F*: 5 sequential frames showing collapse of the wave break at the boundary. Time (in seconds) is shown in each frame.

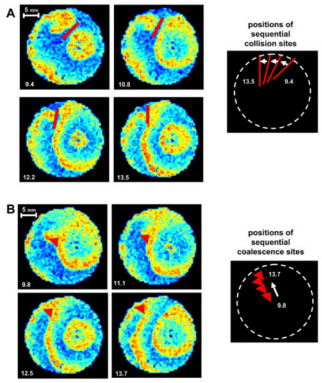

Fig. 8.

Paced-induced movements of collision and coalescence sites. *A*: sequential frames illustrate movement of the collision site (red bar). *B*: sequential frames illustrate movement of a point where the 2 waves coalesce (red triangle). Corresponding cartoons are shown at *right*. Time (in seconds) is shown in each frame.